Catalysis Today 147 (2009) 179–185

Contents lists available at ScienceDirect

Catalysis Today

journal homepage: www.elsevier.com/locate/cattod

Changing the hydroisomerization to hydrocracking ratio of long chain alkanes by varying the level of delamination in zeolitic (ITQ-6) materials

Antonio Chica, Urbano Diaz, Vicente Fornés, Avelino Corma *

Instituto de Tecnología Química, CSIC, UPV, Avda. de los Naranjos s/n, 46022 Valencia, Spain

ARTICLE INFO

Article history:
Available online 16 December 2008

Keywords:
ITQ-6
Hydroisomerization/hydrocracking
Zeolites
n-Hexadecane

ABSTRACT

Several delaminated ITQ-6 acid samples have been synthesized and tested in the isomerization of *n*-hexadecane. It has been found that the swelling time is a decisive parameter to prepare ITQ-6 catalytic materials with different ratios of micro to mesoporous surface area. *n*-Hexadecane hydroisomerization results indicate that the appropriate control of the delamination conditions can drive to obtain optimized ITQ-6 materials highly active for the hydroisomerization/hydrocracking of long chain alkanes to produce lube oils, diesels or gasolines.

1. Introduction

The hydroconversion of *n*-alkanes on bifunctional acid/metal catalysts are important process in oil refining and for the conversion of Fischer-Tropsch products [1–4]. Isomerization of short chain *n*-alkanes is important for enhancing the octane number of gasoline and for improving the low-temperature behaviours ("pour point") of diesel fuels and lubricating oils [5–9]. Bifunctional catalysts containing metallic sites for hydrogenation/dehydrogenation reaction and acidic sites for carbon–carbon bond rearrangement are known to be very effectives in the isomerization of *n*-paraffins [10]. However, at medium to high conversion levels isomerization is always accompanied by hydrocracking and, thus, the yield of isomerised products is limited [11]. Hydrocracking is faster for multibranched than for monobranched alkanes [12–15], and to limit this process it is necessary to suppress the formation of multibranched isomers or to find catalyst that can work at lower temperatures in where the thermodynamics will be relatively more favourable to the formation of multibranched instead of monobranched isomers.

The use of molecular sieve as catalysts can have an impact on isomerization selectivity provided pore dimensions, pore topology, acidity, crystallite size, and adsorption properties are controlled [16–19]. Pore dimensions and topology can be modulated in order to enhance the isomerization of *n*-alkanes through shape selectivity. For instance, 10 ring unidirectional pore zeolites, which avoid the formation of multibranched isomers (with three or more methyl groups), have been successfully used to carry out the isomerization of long normal paraffins with high selectivity to monobranched and dibranched products [20–27].

From the point of view of catalyst acidity, improved selectivity towards middle distillates can be attained by reducing the density of Brønsted acid sites, that is, by increasing the Si/Al ratio [28,29] or by decreasing their acid strength, while increasing the activity of the hydrogenating function [30]. However, the gain in selectivity obtained after reducing the zeolite acidity is always accompanied by a decrease of the catalyst activity, thus requiring higher reaction temperatures or larger contact times to achieve a given degree of conversion [30,14].

Up today, the most suitable catalysts for mild hydrocracking including hydrocracking of Fischer-Tropsch paraffinic feeds to yield middle distillates is amorphous silica–alumina with a hydrogenating function. Zeolites with more diffusional constrains than amorphous silica–alumina are more actives and give, in general, a deeper hydrocracking and are the preferred catalysts for producing more kerosene and naphtha. From the point of view of hydroisomerization and hydrocracking it would be of much interest to find solid catalysts with the pore accessibility of amorphous silica–alumina and the acidity of zeolites. A potential lead in that direction can be the synthesis of layered zeolites, which are subsequently delaminated, making accessible through the external surface all the potential catalytic active sites [31]. Using this approach we have synthesized a zeolitic material, ITQ-6 [32,33], obtained by delamination of layered zeolite precursors (PREFER) having FER-type (Ferrierite) structure [34–36]. The delaminated zeolite is mostly formed by single zeolitic layers

* Corresponding author.
E-mail address: acorma@itq.upv.es (A. Corma).

0920-5861/$ – see front matter © 2008 Elsevier B.V. All rights reserved.
doi:10.1016/j.cattod.2008.10.046

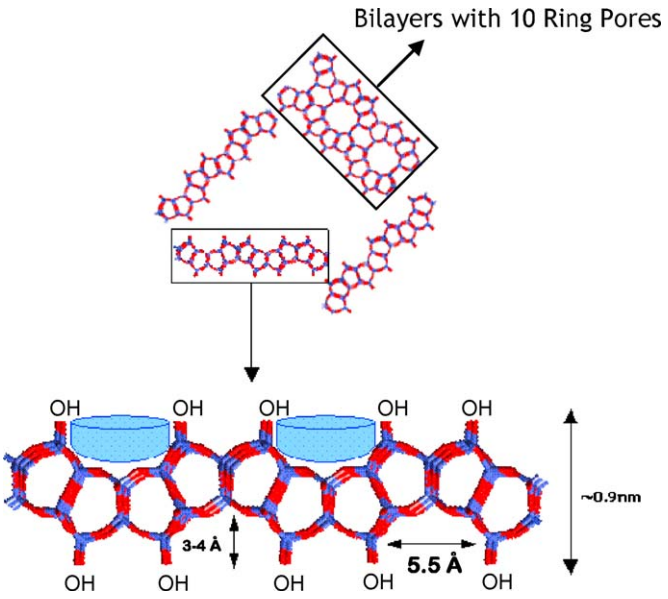

Fig. 1. Artistic representation of ITQ-6, showing the structural details of individual layer of ferrieritic nature.

organized in a "house of card"-type structure with a high external surface area, usually above 600 $m^2\ g^{-1}$. A schematic representation of the ITQ-6 structures is shown in Fig. 1. A fully delaminated PREFER will show only external surface formed by "cups" with ~5.5 Å diameter and 3–4 Å deep. However, if delamination is not completed and the material still presents bi- or trilayers, 10 ring pores will also be present in the partially delaminated material (see Fig. 1).

ITQ-6 could be an interesting hydroisomerization/hydrocracking catalyst since it can, at least theoretically, go from an structured material with no micropores but very large external surface which allows easy access of the reactants to the active site and a good metal dispersion for producing the required bifunctional catalyst, to materials with a tunable ratio of external/microporous surface area.

Here we have studied the effect of the level of delamination on the catalytic performance of this material for *n*-hexadecane hydroisomerization–hydrocracking, showing that the control of the delamination process allows to synthesize an optimized ITQ-6 material with excellent physico-chemical properties for hydroisomerization/hydrocracking of long chain alkanes.

2. Experimental

2.1. Catalysts preparation

The ITQ-6 sample was prepared as follows: 10 g of silica (Aerosil 200, Degussa), 2.3 g of alumina (boehmite, Catapal B), 9.2 g of NH_4F (Aldrich, 98% purity), 3.1 g of HF (Aldrich, 49.8% concentration), 26 g of 4-amino-2,2,6,6-tetramethylpiperidine (Fluka, 98% purity), and 27.9 g of MiliQ deionized water were mixed in an autoclave at 448 K for 5 days. The resulting product, after it was filtered, washed three times with water, and dried at 333 K, had an X-ray diffraction (XRD) pattern characteristic of layered zeolitic precursor PREFER. This material was suspended in a water solution of cetyltrimethylammonium bromide ($CTA^+\ Br^-$) and tetrapropylammonium hydroxide (TPA^+OH^-) and refluxed during different time periods (from 16 to 48 h) at 368 K to obtain an expanded material. Delamination was performed by placing the slurry in an ultrasound bath (50 W, 40 kHz) for 1 h, maintaining a pH of 12.5 and 323 K. Finally, the solid phase was washed thoroughly with water, dried at 373 K, and calcined at 853 K for 7 h yielding typical ITQ-6 delaminated materials with different delamination levels. A portion of PREFER was calcined at 853 K without previous treatment to yield the 3D Ferrierite zeolite.

Incorporation of platinum was accomplished by incipient wetness impregnation of the respective supports with an aqueous solution containing the required amount of H_2PtCl_6 (Aldrich, 99%) to achieve a nominal concentration of 1 wt% platinum in the final catalysts. The solid was further dried at room temperature for 16 h. Finally, all Pt-supported catalysts were calcined in muffle oven at 773 K for 3 h.

2.2. Characterization techniques

Powder XRD data of the materials were recorded in a Philips X'Pert MPD diffractometer equipped with a PW3050 gioniometer (Cu Kα radiation, graphite monochromator) provided with a variable divergence slit.

The platinum content in the calcined catalysts was determined by atomic absorption spectrophotometry (AAS) in a Varian Spectra A-l0 Plus apparatus.

Textural properties of the supports and Pt-containing catalysts were obtained from the nitrogen adsorption isotherms determined at 77 K in a Micromeritics ASAP 2000 equipment. Surface areas were calculated by the BET method and the pore-size distributions were obtained using the BJH formalism. Prior to the adsorption measurements the samples were outgassed at 673 K for 24 h.

The total amount of Brønsted and Lewis acid sites, as well as the acid strength distribution, were determined by room temperature adsorption and thermal desorption of pyridine following the procedure described previously [37]. In those experiments, the samples were first treated in vacuum at 673 K and 0.013 Pa overnight. Then 650 Pa of pyridine were admitted at room temperature and allowed to equilibrate with the sample for 1 h. Subsequently, the sample was evacuated at 523 K and 0.013 Pa for 1 h to remove the physically adsorbed pyridine, and the IR spectrum was recorded at room temperature. The same protocol was repeated after evacuation at 623 and 673 K. The extinction coefficients of Emeis were used to quantify the results [38].

2.3. Catalytic activity

The hydroconversion of *n*-hexadecane (Aldrich, >99%) was carried out in a continuous down flow tubular reactor at a total pressure of 4.0 MPa, $H_2/n\text{-}C_{16}$ molar ratio of 50, and WHSV of 3.6 h^{-1}. The $n\text{-}C_{16}$ conversion was varied by changing the reaction temperature. Typically, the reactor was loaded with 1.0 g of catalyst with a particle size of 0.2–0.4 mm diluted with SiC (0.6–0.8 mm particle size) until a constant volume of 5 cm^3. Before starting the catalytic experiments, catalysts were reduced in situ by passing a flow of pure H_2 (100 cm^3/min) through the reactor at atmospheric pressure and 673 K for 2 h. After the reduction step, the temperature was lowered to the desired reaction temperature, the total pressure increased to 4.0 MPa and the H_2 flow rate adjusted to attain the required $H_2/n\text{-}C_{16}$ ratio. Pure *n*-hexadecane was fed by means of a high-precision HPLC pump (Gilson 305) at the flow rate of 3.6 g/h. The stream leaving the reactor was depressurized and analyzed on-line in a GC (Varian 3400) equipped with a capillary column (Petrocol DH50 cross-linked methylsilicone column, 50 m × 0.32 mm, 1.05-μm film, Supelco) and a flame ionization detector (FID).

The reactor conditions were maintained until a nearly constant composition of the reaction products (pseudo-stationary state) was observed before setting the reactor temperature to a new

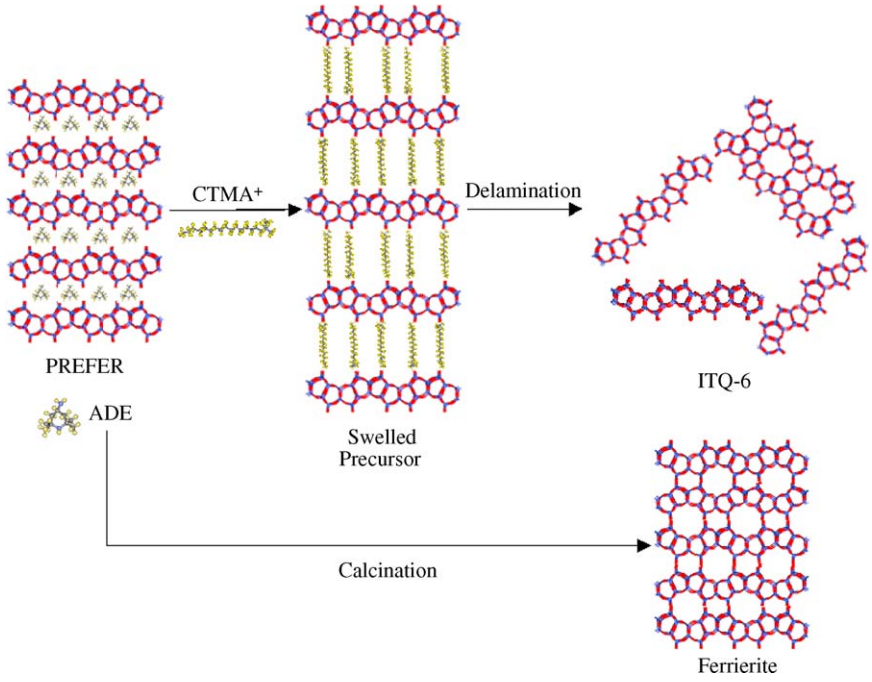

Fig. 2. Schematic representation for the preparation of ITQ-6.

value. At the end of the experiment, the initial reaction conditions were re-established to verify the absence of significant catalyst deactivation. All the catalytic data given in this work correspond to those obtained in the pseudo-stationary state, which was typically attained after about 2 h on stream.

Hexadecane conversion is defined as the percentage of *n*-hexadecane feed that disappeared during the reaction. Product selectivities are reported on a carbon basis as the percentage of the converted *n*-hexadecane appearing as each product. Product yields are reported as the percentage in which each product is presented in the outlet stream.

3. Results and discussion

3.1. Synthesis and characterization of different ITQ-6 samples

The Ferrierite (FER) is a medium pore zeolite containing linked [5^4] polyhedral units having intersecting channels outlined by 10 ring with 0.43 nm × 0.55 nm and 8 ring with 0.34 nm × 0.48 nm pore dimensions. This zeolite presents very interesting acid characteristics, but the reduced pore dimensions only allow the processing of linear and monobranched olefins and paraffins. To increase its potential catalytic applications, it would be of interest to make the acid sites more accessible to reactants. This could in principle be done if a layered precursor could be synthesized. Then, in a first step a laminar precursor of Ferrierite, the PREFER, was synthesized following [39]. After that, the laminar precursor was expanded by using cetyl-trimethylammonium hydroxide (CTMAOH) and TMAOH at pH 12.5. Then the swelled material was delaminated by means of ultrasounds. A scheme of the preparation process is given in Fig. 2 while Table 1 shows the delamination conditions and the Si/Al ratio of the different ITQ-6 samples studied in this work.

The XRD patterns of the starting layered precursor and the expanded material are given in Fig. 3a and b, respectively. It can be seen there that CTMAOH was incorporated between the layers of the FER structure giving a d_{100} spacing of 3.6 nm. Ultrasounds allows the delamination of the structure, which after calcination at 853 K becomes ITQ-6. The XRD pattern of ITQ-6 (Fig. 3c) compared with that of the Ferrierite, obtained after calcination of PREFER at 853 K (Fig. 3d), shows that while the intensities of the reflections corresponding to planes (*0 k l*) were basically unchanged, those corresponding to (*h* 0 0) have strongly decreased in ITQ-6. This indicates a remarkable loss of order along the *a*-axis, which would

Table 1
Preparation conditions and chemicals analyses of different ITQ-6 samples.

Sample	Swelling time (h)	$(Si/Al)_{exp}$[a]
FER	0	30
$(ITQ\text{-}6)_{16}$	16	34
$(ITQ\text{-}6)_{36}$	36	48
$(ITQ\text{-}6)_{48}$	48	64

[a] Si/Al molar ratios obtained from chemical analysis using atomic absorption.

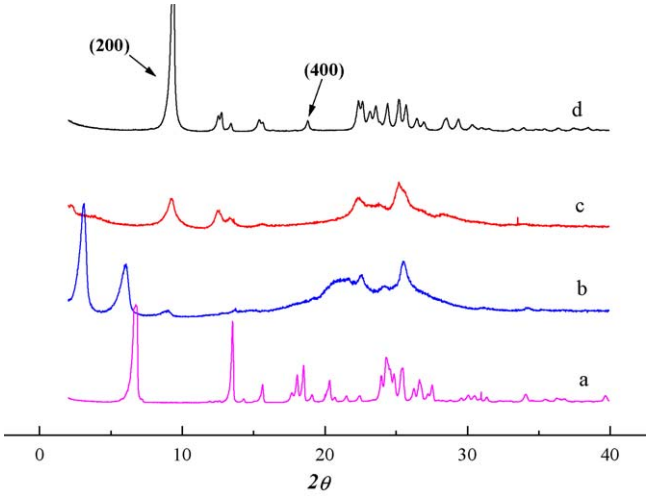

Fig. 3. XRD patterns of PREFER (a), swollen material after 16 h of treatment (b), ITQ-6 calcined (c), and Ferrierite (d).

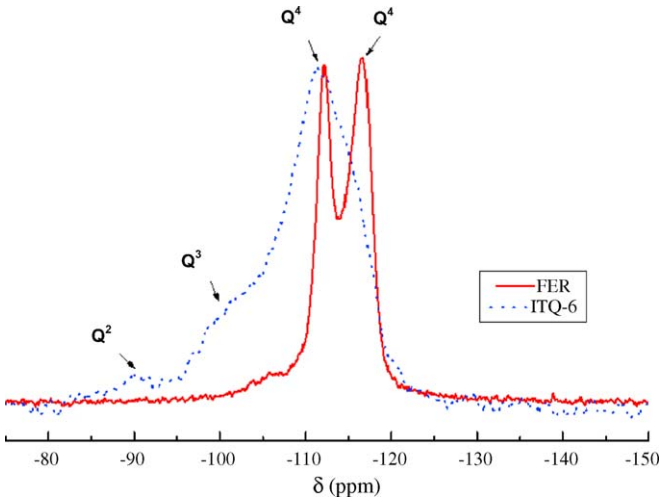

Fig. 4. ^{29}Si MAS NMR spectra of ITQ-6 and Ferrierite.

be consistent with a delamination of the layered PREFER. Different levels of delamination can be achieved by changing the time of swelling for the PREFER. Thus, results form Table 2 show that by controlling this preparation variable it is possible to change significantly the ratio of external to microporous surface area. In fact, a sample was produced that shows no microporosity but 882 $m^2\ g^{-1}$ of external surface area.

The delamination of the PREFER should produce a large number of surface silanols. Indeed, a delaminated material like ITQ-6 should present a high ratio of Q^3 (Si2SiOH)/Q^4(Si4Si) in where Q^3 atoms would mainly correspond to terminal $(Si_3)SiOH$. From the ^{29}Si MAS NMR spectra of ITQ-6 and Ferrierite one can see in the former a much larger proportion of Q^3 species (−100 ppm) as well as the presence of Q^2 geminal groups (−92 ppm), $(Si_2)Si(OH)_2$, at the vertexes of the ITQ-6 layers (see Fig. 4). The formation of a large amount of Q^3 and Q^2 groups is also consistent with the silanol groups present in ITQ-6 as detected by IR spectroscopy (bands at 3740 and 960 cm^{-1}) (see Fig. 5). A certain level of dealumination is also occurring during delamination as indicated by the chemical analysis results (see Table 1). The decrease of the Al content has a direct influence on the acidity of the samples. Indeed, pyridine adsorption results indicate that, in general, the Brønsted acidity, which is associated to the presence of bridged hydroxyl groups decreases when increasing the level of delamination (see Table 3), being especially noticeable for the most delaminated ITQ-6 sample $(ITQ\text{-}6)_{48}$.

Pyridine desorption at different temperatures allow to distinguish the population of acid sites with different strengths. Only the strongest acid sites will retain pyridine at the highest desorption temperature (673 K). It is remarkable that the delaminated ITQ-6 samples have still a large number of the very strong Brønsted acid sites (see Table 3).

At this point we have a set of samples that have different level of accessibility for the reactants and different amount of potential active sites. This occurs in such a way that the samples with larger external surface area (higher accessibility, less diffusional problems) have a lower number of active sites. Will see now how these two variables, with potential opposite effect, influence the final catalytic behaviour for hydroisomerization and hydrocracking.

3.2. n-Hexadecane hydroisomerization–hydrocracking conversion

n-C_{16} conversions are plotted in Fig. 6 as a function of reaction temperature. The results clearly show that all the ITQ-6 samples

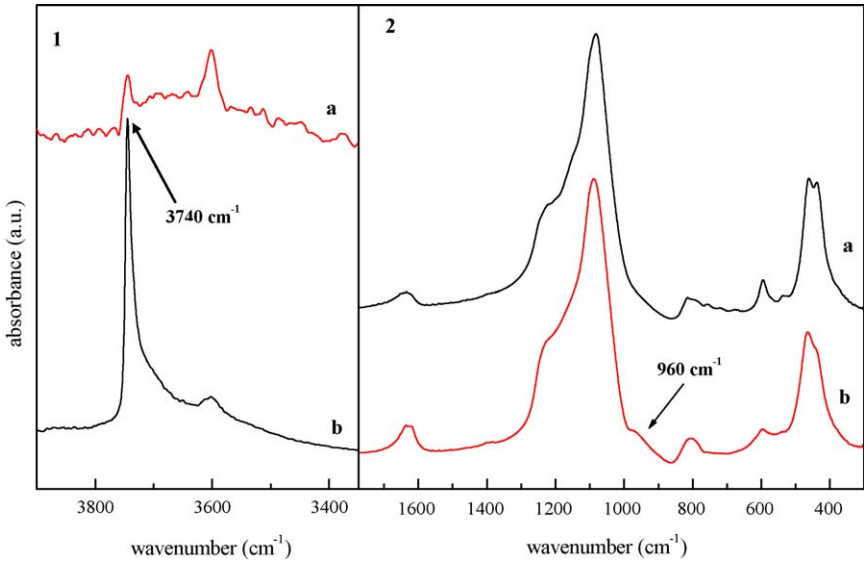

Fig. 5. IR spectra in the region of (1) hydroxyl stretching vibrations and (2) framework Si–O stretching vibrations for (a) Ferrierite obtained by calcination of PREFER and (b) ITQ-6 obtained by delamination of PREFER.

Table 2
Textural properties of ITQ-6 samples with different delamination levels.

Sample	S_{BET} ($m^2\ g^{-1}$)	S_{MIC} ($m^2\ g^{-1}$)	S_{EXT} ($m^2\ g^{-1}$)	V_{TOT} ($cm^3\ g^{-1}$)	V_{MIC} ($cm^3\ g^{-1}$)	V_{MESO} ($cm^3\ g^{-1}$)
FER	277	225	52	0.195	0.113	0.058
$(ITQ\text{-}6)_{16}$	532	72	454	0.562	0.047	0.342
$(ITQ\text{-}6)_{36}$	605	53	552	0.686	0.028	0.651
$(ITQ\text{-}6)_{48}$	882	0	882	0.786	0	0.754

Table 3
Acidity measurements of ITQ-6 samples after adsorption–desorption of pyridine molecules. The results correspond to μmol Py for each gram of solid sample using Emeis adsorption coefficients [37] for the bands assigns to Lewis (1455 cm^{-1}) and Brönsted (1545 cm^{-1}) acid sites.

Sample	523 K		623 K		673 K	
	Lewis	Brønsted	Lewis	Brønsted	Lewis	Brønsted
FER	6.8	61.5	6.8	49.6	3.4	11.9
$(ITQ\text{-}6)_{16}$	19.8	39.7	17.4	31.8	12.5	22.8
$(ITQ\text{-}6)_{36}$	10.6	41.7	12.1	34.7	10.6	21.8
$(ITQ\text{-}6)_{48}$	9.1	19.9	7.6	16.9	4.5	7.9

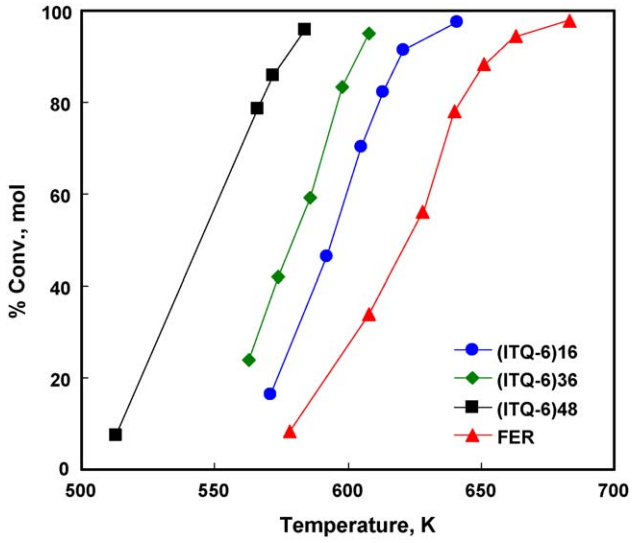

Fig. 6. Conversion of *n*-hexadecane over Ferrierite and ITQ-6 catalyts versus reaction temperature. *Reaction conditions*: total pressure of 4 MPa, H_2/hexadecane ratio of 50 mol/mol and contact time of 0.279 h.

give a higher conversion than Ferrierite, indicating that the gain in accessibility due to delamination is more important than the amount of acid sites lost during delamination. This conclusion also applies within the family of ITQ-6 samples, since $(ITQ\text{-}6)_{48}$ with the highest Si/Al ratio (Si/Al = 64) and the lowest acidity, is the most active one.

From the above we can conclude that *n*-C_{16} should already be diffusional limited within the 10 ring unidimensional pore zeolite (Ferrierite), and the delamination strongly increases the accessibility of the reactant to the acid sites up to the point that it can overcompensate the loss of framework aluminium, and therefore the loss of Brønsted acidity, that occurred during delamination.

3.3. *n*-Hexadecane hydroisomerization/hydrocracking selectivity

Fig. 7 presents the yields to hydroisomerization and hydrocracking at different levels of conversion. In a first approximation it can be seen there three different groups of samples. Firstly the most delaminated $(ITQ\text{-}6)_{48}$ that gives almost no isomers but cracking products. The second group corresponds to Ferrierite and $(ITQ\text{-}6)_{36}$, with a higher ratio of isomerization to cracking with respect to $(ITQ\text{-}6)_{48}$ (see Table 4). Finally $(ITQ\text{-}6)_{16}$, which is the less delaminated, gives the highest selectivity to hydroisomerization, being this especially visible at higher levels of conversion.

The ratio of monobranched/(di- + tribranched) for Ferrierite, shown in Table 4, is similar to the unidimensional mediumpore samples such as, for instance, those with TON structure ($\theta - 1$ and ZSM-22) or SAPO-11. These materials are excellent catalysts for

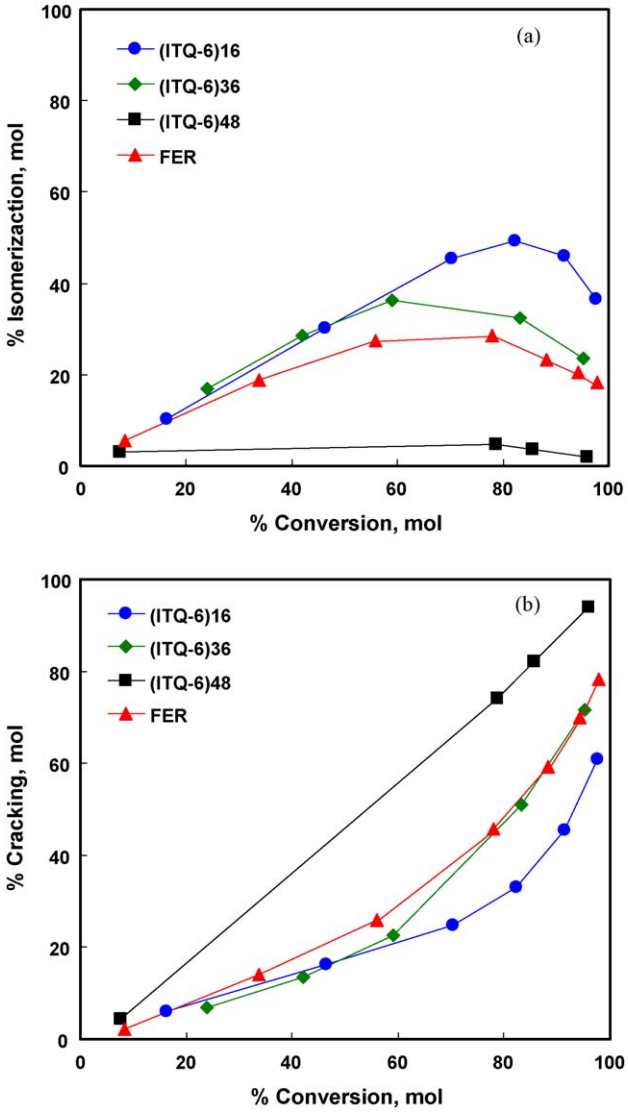

Fig. 7. Isomerization (a) and cracking (b) versus conversion of *n*-hexadecane over Ferrierite and ITQ-6 catalyts. *Reaction conditions*: total pressure of 4 MPa, H_2/hexadecane ratio of 50 mol/mol, and contact time of 0.279 h.

producing lubes by isomerization of long chain paraffins [40]. Indeed, the results presented in Fig. 8 show that these zeolites give high isomerization selectivity with a large ratio of mono- to di-plus tribranched products (see also Table 4). In the case of the

Table 4
Monobranched/(di- + tribranched) isomers ratio and isomerization/cracking yield ratio for the ITQ-6 samples and different catalysts obtained in the isomerization of *n*-hexadecane. *Reaction conditions*: total pressure of 4 MPa, H_2/hexadecane ratio of 50 mol/mol and contact time of 0.279 h.

Catalyst	$[M/(D+T)]$[a]	Isomer./crack.[a]	Reaction *T* (K)[a]
FER	3.5	1.2	625
$(ITQ\text{-}6)_{16}$	1.7	2.1	600
$(ITQ\text{-}6)_{36}$	1.2	1.5	578
$(ITQ\text{-}6)_{48}$	–	0.1	552
ZSM-22	3.8	4.0	555
SAPO-11	3.0	4.5	655
Beta	0.9	15.7	503
SSZ-33	1.0	9.2	502
SSZ-24	1.2	6.1	573

[a] Data obtained at 60% of conversion of *n*-hexadecane.

Table 5
Isomers distribution selectivity obtained in the hydroisomerization of *n*-hexadecane with FER and delaminated ITQ-6 samples. *Reaction conditions*: total pressure of 4 MPa, H_2/hexadecane ratio of 50 mol/mol and contact time of 0.279 h.

	Sample						
	FER		$(ITQ\text{-}6)_{16}$		$(ITQ\text{-}6)_{36}$		$(ITQ\text{-}6)_{48}$
	613 K[a]	633 K[a]	583 K[a]	613 K[a]	568 K[a]	598 K[a]	566 K[a]
% Conversion	30	80	30	80	30	80	80
% Isomerization	12.5	32.2	20.8	49.3	22.0	31.5	4.4
% Isomer. selec.	41.7	40.3	69.3	61.6	73.3	39.4	5.5
% 2-MB	22.4	18.9	12.0	9.5	9.1	8.9	15.9
% 3-MB	18.4	17.4	11.1	9.3	10.0	8.3	15.9
% 4-M	11.2	10.9	9.6	9.1	10.9	7.3	13.6
% 5-MB	12.0	9.9	10.6	9.1	11.4	7.9	13.6
% 6-MB	8.0	8.4	11.1	7.9	11.8	6.7	11.4
% (7 + 8)MB	21.6	23.0	26.4	17.2	20.5	15.2	29.5
(2 + 3)/(4 + 5 + 6 + 7 + 8)	0.77	0.70	0.40	0.43	0.35	0.46	0.47
% DM	6.4	11.2	18.3	28.4	25.0	26.3	0.0
% TB	0.0	0.3	1.0	9.3	1.4	19.4	0.0

Note: MB, monobranched; DB, dibranched; TB, tribranched.
[a] Reaction *T*.

Ferrierite it is not an unidirectional zeolite since the 10 ring channels are connected by 8 ring pores. This is probably the reason why Ferrierite shows lower isomerization selectivity and lower isomerization to cracking ratio than TON (ZSM-22) and SAPO-11 (see Table 4). However, the 10 ring main pore has a clear influence on the ratio of mono- to di- plus tribranched isomers. In fact, results presented in Table 4 show that the ratio is not different for Ferrierite, TON (ZSM-22), and SAPO-11. On the contrary, highly delaminated samples give a lower $M/(D + T)$ ratio, which become closer to the values observed (see Table 4) for zeolites such as Beta, SSZ-33, and SSZ-24 with large pores in where there is not shape selectivity control.

The location of the methyl group within the methyl pentadecane isomers, also depends on pore topologies and dimensions [18,19]. With Ferrierite, 2- and 3-methtyl pentadecane are preferentially formed over the whole conversion level (see Table 5). It has been reported that the 3- and especially the 2-methyl isomers are clearly favoured in zeolites with channels formed by 10 ring [41]. Then, if we accept that monomethyl isomers are formed mainly inside the pores and moreover that the *n*-alkane–*n*-alkene should diffuse in single file with the molecule elongated, it appears that the isomerization at the second and third carbons should preferentially occur from a geometrical point of view in Ferrierite [19,27]. In addition, the higher product selectivity to 2-methyl pentadecane with respect to the other monobranched isomers can also be due to the larger intracrystalline diffusivity of the former, as has been calculated by Webb et al. [42,43]. If one looks closely at the monobranched isomer distribution (Table 5) it appears that the ratio of (C2–C3–MB)/(C4–C5–C6–C7–C8–MB) methyl pentadecane isomers decreases when increasing the degree of delamination. This would support the conclusion that 4-, 5-, 6-, 7-, and 8-monobranched isomers are formed preferentially at the external surface, either directly of by methyl shift isomerization of 2- and 3-methyl pentadecane.

Methane and pentadecane were not observed in the hydrocracked products formed over all samples, indicating that hydrogenolysis over the Pt centres did not occur to any appreciable extent. The molar distribution of cracking products grouped by carbon number obtained for all catalysts is shown in Fig. 9, at 80% of *n*-hexadecane conversion. Important differences in the distribution of the hydrocracked products were observed between

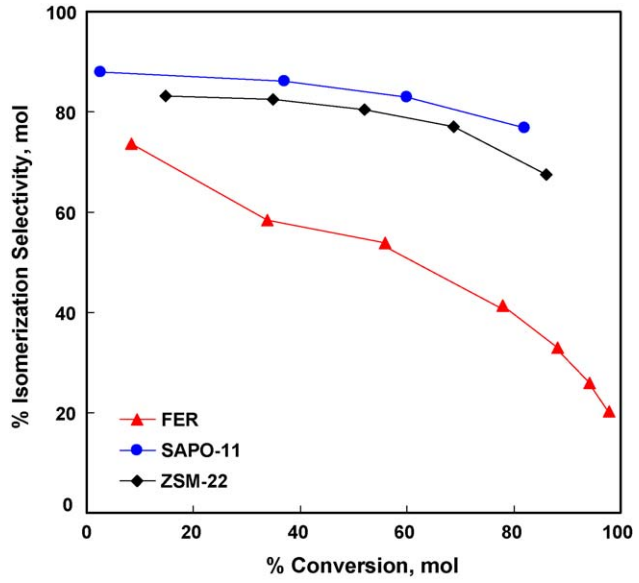

Fig. 8. Isomerization selectivity of Ferrierite, SAPO-11 and ZSM-22 materials in the hydrosiomerization of *n*-hexadecane. *Reaction conditions*: total pressure of 4 MPa, H_2/hexadecane ratio of 50 mol/mol and contact time of 0.279 h.

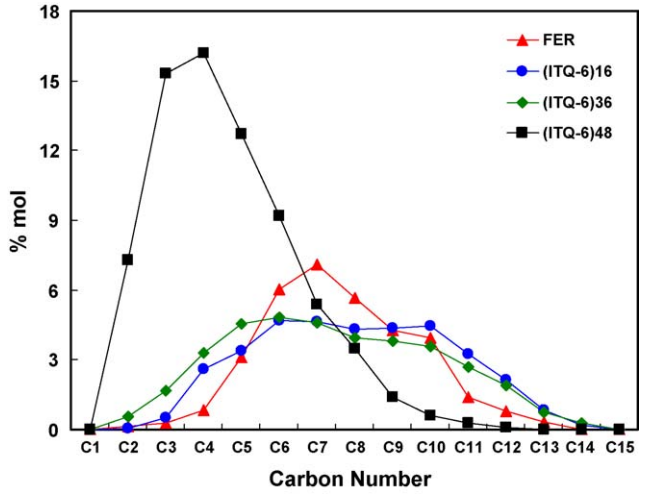

Fig. 9. Cracking products distribution conversion of *n*-hexadecane over Ferrierite and ITQ-6 catalyts. *Reaction conditions*: total pressure of 4 MPa, H_2/hexadecane ratio of 50 mol/mol, contact time of 0.279 h, and 80% of conversion level.

delaminated samples and the reference material (Ferrierite). Indeed, Ferrierite gives a cracking product distribution centred at C7 (gasoline range), while delaminated materials $(ITQ\text{-}6)_{16}$ and $(ITQ\text{-}6)_{36}$ gave a rather broad distribution. Cracking products distribution for $(ITQ\text{-}6)_{48}$ is centred at C3–C4. As observed, the distribution obtained for $(ITQ\text{-}6)_{48}$ was completely asymmetric, indicating that secondary cracking was taking place in larger extension over the most delaminated ITQ-6 materials.

4. Conclusions

It has been found that it is possible to control the extension of delamination of the PREFER layered precursor of Ferrierite through the time dedicated to swell this precursor by intercalation of a larger cationic molecule. Then, acid solids formed by well-structured single or condensed layers with variable ratios of external to internal (micropore) surface area can be achieved. With these materials is possible to prepared bifunctional acid/metal catalysts with a hydroisomerization to hydrocracking ratio and an isomers distribution that can cover a continuous range from the catalytic behaviour of the purely 10 ring to the extra large pore zeolites. The very highly delaminated zeolites may be used at low operation temperatures where the commercial amorphous silica–alumina materials exhibit modest activity.

References

[1] M. Steijns, G. Froment, P.A. Jacobs, J. Uytterhoeven, J. Weitkamp, Ind. Eng. Chem. Prod. Res. Dev. 20 (1981) 654.
[2] J. Weitkamp, P.A. Jacobs, J.A. Martens, Appl. Catal. 8 (1983) 123.
[3] J. Weitkamp, W. Gerhardt, P.A. Jacobs, Acta Phys. Chem. 31 (1985) 31.
[4] J. Weitkamp, Stud. Surf. Sci. Catal. 7 (1981) 1404.
[5] A. Chica, A. Corma, P.J. Miguel, Catal. Today 65 (2001) 101.
[6] A. Chica, A. Corma, J. Catal. 187 (1999) 167.
[7] S.J. Miller, Stud. Surf. Sci. Catal. 84 (1994) 2319.
[8] A.P.E. York, C. PhamHuu, P. DelGallo, M.J. Ledoux, Catal. Today 35 (1997) 51.
[9] P. Delporte, C. PhamHuu, M.J. Ledoux, Appl. Catal. A 149 (1997) 151.
[10] J. Weitkamp, Ind. Eng. Chem. Prod. Res. Dev. 21 (1982) 550.
[11] J.A. Martens, P.A. Jacobs, J. Weitkamp, Appl. Catal. 20 (1986) 239.
[12] A. Chica, A. Corma, Chem. Ing. Tech. 79 (2007) 857.
[13] J. Weitkamp, P.A. Jacobs, Abs. Pap. Am. Chem. Soc. 181 (1981) 13-PETR.
[14] F. Alvarez, F.R. Ribeiro, G. Perot, C. Thomazeau, M. Guisnet, J. Catal. 162 (1996) 179.
[15] A. Patrigeon, E. Benazzi, Ch. Travers, J.Y. Bernhard, Catal. Today 65 (2001) 149.
[16] A. Corma, J. Catal. 216 (2003) 298.
[17] D.S. Santilli, S.I. Zones, Catal. Lett. 7 (1990) 383.
[18] B. Smit, T.L.M. Maesen, Nature 451 (2008) 671.
[19] T.L.M. Maesen, E. Beerdsen, S. Calero, D. Dubbeldam, B. Smit, J. Catal. 237 (2006) 278.
[20] S.J. Miller, Micropor. Mater. 2 (1994) 39.
[21] F.G. Dwyer, E.W. Valyocsik, US Patent 5,336,478 (1994), to Mobil Oil Corp.; D.J. Klocke, J.C. Vartuli, G.W. Kirker, EP Patent 220,893 A2 (1987), to Mobil Oil Corp.
[22] M.C. Claude, G. Vanbutsele, J.A. Martens, J. Catal. 203 (2001) 213.
[23] W.J. Ball, S.A.I. Barri, D. Young, EP Patent 104,800 A1 (1984), to British Petroleum.
[24] T. Blasco, A. Chica, A. Corma, W.J. Murphy, J. Agúndez-Rodríguez, J. Pérez-Pariente, J. Catal. 242 (2006) 153.
[25] C.M. Claude, J.A. Martens, J. Catal. 190 (2000) 39.
[26] J.A. Martens, G. Vanbutsele, P.A. Jacobs, J. Denayer, R. Ocakoglu, G. Baron, J.A. Muñoz-Arroyo, J. Thybaut, G.B. Marin, Catal. Today 65 (2001) 111.
[27] G. Sastre, A. Chica, A. Corma, J. Catal. 195 (2000) 227.
[28] R. Bezman, Catal. Today 13 (1992) 143.
[29] J.A.R. Van Veen, in: M. Guisnet, J.P. Gilson (Eds.), Zeolites for Clearner Technologies, Imperial College Press, 2002, p. 131 (Chapter 6).
[30] J.A. Martens, M. Tielen, P.A. Jacobs, in: H.G. Karge, J. Weitkamp (Eds.), Zeolites as Catalysts, sorbents and Detergent, Stud. Surf. Sci. Catal., vol. 49, Elsevier, Amsterdam, 1989, p. 49.
[31] A. Corma, V. Fornés, J. Martinez-Triguero, S.B. Pergher, J. Catal. 186 (1999) 57.
[32] A. Corma, U. Diaz, M.E. Domine, V. Fornés, Angew. Chem. Int. Ed. 39 (2000) 1499.
[33] A. Corma, A. Chica, U. Díaz, V. Fornés. World Patent WO200007722-A (2000), to BP Oil Int.
[34] R. García, L. Gómez-Hortigüela, I. Díaz, E. Sastre, J. Pérez-Pariente, Chem. Mater. 20 (2008) 1099.
[35] R. Millini, L.C. Carluccio, A. Carati, G. Bellussi, C. Perego, G. Cruciani, S. Zanardi, Micropor. Mesopor. Mater. 74 (2004) 59.
[36] L. Schreyeck, P. Caullet, J.C. Mougenel, J.L. Guth, B. Marler, Micropor. Mater. 6 (1996) 259.
[37] A. Corma, V. Fornés, E. Ortega, J. Catal. 92 (1985) 284.
[38] C.A. Emeis, J. Catal. 141 (1993) 347.
[39] L. Schereyeck, P. Caullet, J.C. Mougenel, J.L. Guth, B. Marler, Chem. Commun. 21 (1995) 2187.
[40] S.J. Miller, J. Xiao, J.M. Rosenbaum, Science and Technology in catalysis, Stud. Surf. Sci. Catal., vol. 92, Elsevier, Amsterdam, 1995, p. 379.
[41] S. Ernst, J. Weitkamp, J.A. Martens, P.A. Jacobs, Appl. Catal. 48 (1989) 137.
[42] E.B. Webb, G.S. Grest, Catal. Lett. 56 (1998) 95.
[43] E.B. Webb, G.S. Grest, M. Mondello, J. Phys. Chem. B 103 (1999) 4949.